Effective Connectivity in Subjects With Mild Cognitive Impairment as Assessed Using Functional Near-Infrared Spectroscopy

Lingguo Bu, PhD, Congcong Huo, BS, Yuexia Qin, PhD, Gongcheng Xu, MD, Yonghui Wang, PhD, and Zengyong Li, PhD

Objective: This study aimed to reveal the physiological mechanism in subjects with mild cognitive impairment based on effective connectivity method.

Methods: Effective connectivity was assessed by dynamic Bayesian inference of the oxygenated hemoglobin concentration signals measured through functional near-infrared spectroscopy. The oxygenated hemoglobin concentration signals were recorded from the left prefrontal cortex, right prefrontal cortex, left motor cortex, right motor cortex, left occipital lobe, and right occipital lobe of 26 subjects with mild cognitive impairment (mild cognitive impairment group) and 28 healthy elderly subjects (control group) at resting state.

Results: The coupling strength of right prefrontal cortex to left prefrontal cortex ($F = 7.964$, $P = 0.007$) and left prefrontal cortex to right occipital lobe ($F = 4.278$, $P = 0.044$) in interval III as well as left prefrontal cortex to left occipital lobe ($F = 5.637$, $P = 0.021$), right occipital lobe to left prefrontal cortex ($F = 4.762$, $P = 0.034$), and right prefrontal cortex to left occipital lobe ($F = 4.06$, $P = 0.049$) in interval IV in the mild cognitive impairment group were significantly lower than those in the control group.

Conclusions: The decreased effective connectivity levels among brain regions may be a marker of impaired cognitive function in the mild cognitive impairment group. The constructed effective connectivity network based on functional near-infrared spectroscopy provide a noninvasive method to assess mild cognitive impairment.

Key Words: Mild Cognitive Impairment, Effective Connectivity, Near-Infrared Spectroscopy

(*Am J Phys Med Rehabil* 2019;98:438–445)

Mild cognitive impairment (MCI) refers to a cognitive decline that is more severe than the expected level of an individual's age and education.[1] Epidemiological studies revealed that MCI is manifested mainly by elderly people older than 65 yrs at a proportion of 10%–20%.[2] Mild cognitive impairment progresses to Alzheimer disease at a conversion rate of 6%–12% per year.[3] The most promising intervention is the early detection of individuals at the prodromal stage of Alzheimer disease. Therefore, objective markers that can reliably distinguish MCI from normal aging must be identified.

Subjective memory complaints are documented in individuals with MCI through abnormal performances in objective cognitive tests.[4] Existing methods for evaluating MCI mainly include the following: (*a*) subjective surveys, such as Mini-Mental State Examination (MMSE),[5] Montreal Cognitive Assessment (MoCA),[6] subjective cognitive complaint,[7] clock-drawing test,[8] and DemTect,[9] all of which are simple and easy to accomplish. Subjective surveys can neither provide an objective measurement data nor be used to assess cognitive processes in real time. Thus, a scale cannot fully diagnose the MCI level; (*b*) physiological parameter detection methods, such as functional magnetic resonance imaging[10] and positron emission tomography[11]; and (*c*) behavioral ability assessment methods, such as reaction capacity.[12] At present, although many approaches are available for evaluating MCI, the accurate, scientific, and effective evaluation of MCI remains a challenge. Thus, objective and quantitative methods must be combined for MCI evaluation.

Cognitive function requires a high level of functional interaction among the regions of a network supporting cognition. Cognitive function is controlled not by a single brain area but by a brain functional network widely distributed in the brain. Functional connectivity (FC) can reflect the internal activity characteristics of the brain.[13] Functional connectivity refers to the dynamic synchronization of neural activity signals in different regions of the brain, which can reveal the synergy among different brain regions.[13] However, FC cannot elucidate the mechanisms of neuronal coupling. Effective connectivity (EC) is explicitly related to the effect exerted by one neural system on another at either a synaptic or a population level. Effective connectivity is dynamic (i.e., activity-dependent) and critical in modeling interactions or coupling.[14]

Functional near-infrared spectroscopy (fNIRS) is a noninvasive neuroimaging technology that provides technical support

From the Department of Physical Medicine and Rehabilitation, Qilu Hospital, Shandong University, Jinan, PR China (LB, YW); Key Laboratory of High Efficiency and Clean Mechanical Manufacture, School of Mechanical Engineering, Shandong University, Jinan, PR China (LB); Beijing Key Laboratory of Rehabilitation Technical Aids for Old-Age Disability, National Research Center for Rehabilitation Technical Aids, Beijing, PR China (CH, GX, ZL); School of Mechanical and Electronic Engineering, Shandong Jianzhu University, Jinan, PR China (YQ); and Key Laboratory of Rehabilitation Aids Technology and System of the Ministry of Civil Affairs, Beijing, PR China (ZL).

All correspondence should be addressed to: Yonghui Wang, PhD, Department of Physical Medicine and Rehabilitation, Qilu Hospital, Shandong University, 107 Wenhua West Rd, Lixia District, Jinan, Shandong Province, China 250012; and Zengyong Li, PhD, National Research Center for Rehabilitation Technical Aids, 1 Ronghuazhong Rd, Beijing Economic and Technological Development Zone, Beijing, China 100176.

YW and ZL contributed equally to this work.

The study was supported by the National Natural Science Foundation of China (NSFC Number 31771071, 61761166007, 11732015, and 81672249) and Fundamental Research Funds for Central Public Welfare Research Institutes (118009001000160001).

Financial disclosure statements have been obtained, and no conflicts of interest have been reported by the authors or by any individuals in control of the content of this article.

ISSN: 0894-9115

DOI: 10.1097/PHM.0000000000001118

for the detection and analysis of cerebral blood oxygen signals.[15] Functional near-infrared spectroscopy can monitor changes in the concentrations of local oxygenated ($\Delta[HbO_2]$) and deoxygenated ($\Delta[HHb]$) hemoglobin.[15] In the study of brain function, fNIRS offers the following advantages[15]: (*a*) nonintrusive, portable, and low cost; (*b*) moderate time resolution and spatial resolution; and (*c*) convenient operation and low demand for the subjects. Thus, fNIRS is suitable for assessing the level of brain function both in elderly and young patients with MCI.

The prefrontal cortex performs advanced neural information processing functions, including memory, judgment, analysis, thinking, and operation.[16] The motor cortex is mainly responsible for coordinating sensory and motor functions.[17] The occipital lobe is crucial in processing visual information and modulated by planning, executing, and imagining movements.[18]

We hypothesized that the MCI people exhibited altered EC networks among brain regions based on the fNIRS and these changes were related to cognitive performance. The findings may provide an evidence for cognitive decline and offer a new method of accessing the cognitive ability in the MCI people.

MATERIALS AND METHODS

Subjects

A total of 54 subjects were recruited from a local community. The research place is at National Research Center for Rehabilitation Technical Aids, PR China. The subjects included 26 individuals with MCI (MCI group) and 28 age-matched individuals (control group). Sample size was a function of the following three factors: the significance level, power, and effect size. Using two tails, the effect size value was defined as 0.8, the significance level was 0.05, the power value was 0.8, and the minimum sample size was 26 in each group after calculation.[19] Based on the subjects in this study, power value was calculated to be 0.82, which can meet the experimental requirements. To minimize the effect of educational level on the scale test results, all subjects in this experiment were guaranteed to have reached at least high school.[6]

All subjects satisfied the following criteria: (*a*) no abnormal brain structure caused by tumor and head trauma to avoid the influence of brain injury and other factors on the experimental results; (*b*) no neurological diseases to eliminate the effect of neurological diseases on the experimental results; (*c*) no smoking or drinking habits; and (*d*) adequate sleep on the night before the test (good sleep quality refers to a series of good sleeping habits, including sleeping no less than 6.5 hrs each night for the past month, going to sleep not later than 1:00 a.m. and waking up not later than 9:00 a.m.).

We combined the clinical history information and cognitive assessment scale provided by the patients and their families to confirm the sample grouping. The MCI subjects or their family members actively reported subjective cognitive decline. The MMSE score was between 24 and 29.[5] The MoCA score was between 22 and 26.[20] The experimental procedure was approved by the Human Ethics Committee of National Research Center for Rehabilitation Technical Aids and was in accordance with the ethical standards specified by the Helsinki Declaration of 1975 (revised in 2008). All participants provided a written informed consent before they participated in the study. The experiment will stop immediately if someone feels any discomfort.

Functional Near-Infrared Spectroscopy Measurement

The $\Delta[HbO_2]$ signals were obtained using a multichannel commercial fNIRS system (Nirsmart; Danyang Huichuang Medical Equipment Co, Ltd, PR China). The used wavelengths were 780, 808, and 850 nm. The sampling rate was 10 Hz. The system has high reliability and strong stability.[21] The subjects were tested in a room without noise. The room temperature was maintained at 22°C. After the personal information and scale test of the subjects were recorded, they relaxed for 10 mins to come down. In this experiment, the $\Delta[HbO_2]$ signals were acquired from the MCI and control groups at resting state for 15 mins. During this process, the subjects were instructed to maintain a comfortable sitting position, remain still, and relax with eyes closed. Figure 1 shows the measurement process of the experiment.

In the current study, each optode was attached to the skull surface by using a custom-made cap and covered with a black cloth to prevent penetration of ambient light (Fig. 2A). The 14 channels of fNIRS were positioned over the left prefrontal cortex (LPFC), right prefrontal cortex (RPFC), left motor cortex (LMC), right motor cortex (RMC), left occipital lobe (LOL), and right occipital lobe (ROL). These channels were contributed by the sensors and the optodes (Fig. 2B). The measurement sites were FP1, FP2, AF3, AF4, FC1, FC2, FC3, FC4, C1, C2, C3, C4, O1, and O2 corresponding to the position of the international general 10/10 electrode distribution system.

Data Preprocessing

The $\Delta[HbO_2]$ signals were firstly processed with the preprocessing method.[21,22] Data preprocessing was used to eliminate outliers and accurately calculate and analyze the signals. Moving average was used to address abnormal signals in the time series. A method based on moving standard deviation and spline

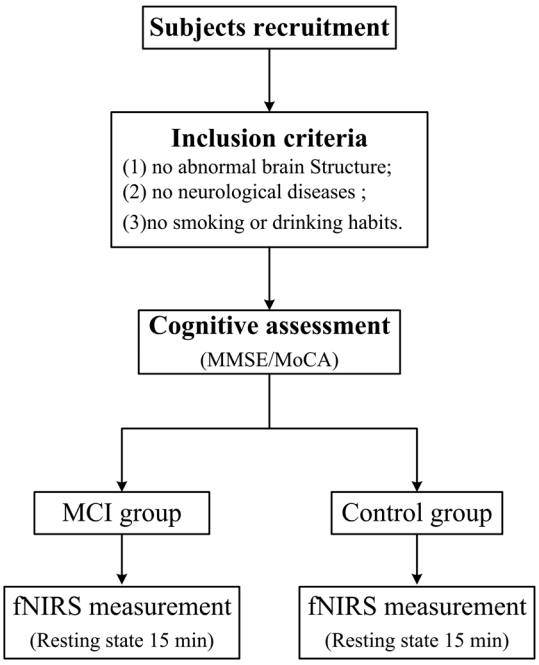

FIGURE 1. The measurement process of the experiment.

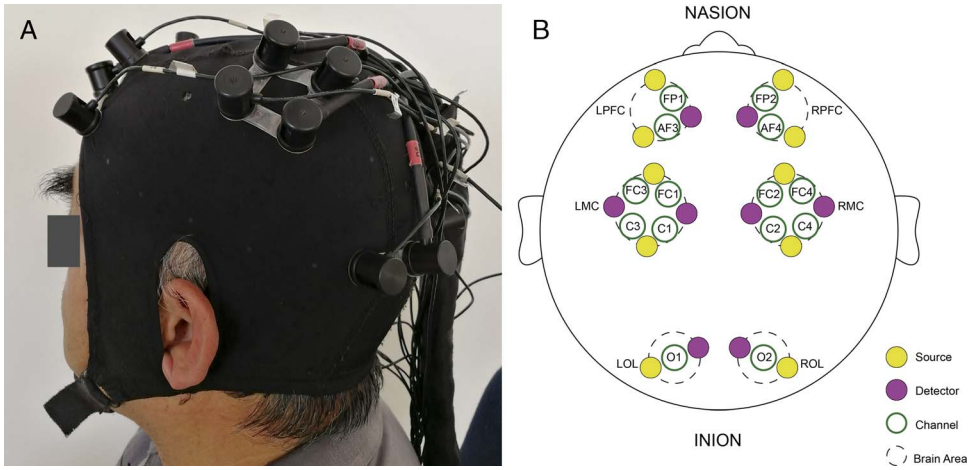

FIGURE 2. Functional near-infrared spectroscopy on a subject (A). Configuration of the measurement channels in the prefrontal cortex, the motor cortex, and the occipital lobe areas according to the international 10/10 system (B).

interpolation was adopted in this study to reduce the movement artifacts.[23] A Butterworth filter was selected to filter noise and interference signals.[21]

Wavelet Transform

The method of wavelet transform[24] converts signals from the time domain into the time-frequency domain. Wavelet transform identifies the time-varying frequency and phase, suggesting that it can be used to analyze nonstationary $\Delta[HbO_2]$ signals. Wavelet transform can provide a time-frequency window that changes with the frequency, and it delivers the phase and amplitude information of the signals at all frequencies and moments. Wavelet transform distinguished five frequency-specific oscillator intervals with potential physiological significance as follows[25]: I: 0.6–2 Hz (cardiac activity); II: 0.145–0.6 Hz (respiratory activity); III: 0.052–0.145 Hz (myogenic activity); IV: 0.021–0.052 Hz (neurogenic activity); and V: 0.0095–0.021 Hz (nitric oxide–related endothelial activity). Figure 3A shows the original $\Delta[HbO_2]$ signal. Figure 3B shows the preprocessed $\Delta[HbO_2]$ signal. Figure 3C shows the average wavelet amplitude in each frequency interval.

Interaction Mechanisms–Coupling Functions Through Bayesian Inference

In this study, the EC of the subjects in the MCI and control groups was assessed by dynamic Bayesian inference (DBI) of the $\Delta[HbO_2]$ signals that were measured through fNIRS. In the life system, biological oscillations are observed at different time scales from microscopic to macroscopic, such as cell signals, cell energy metabolism, and neural networks. The $\Delta[HbO_2]$ signal measured by fNIRS is a complex oscillatory time series, meaning the oscillatory changes in $[HbO_2]$. Coupling functions can describe the dynamical mechanism of interactions between a pair of oscillators.[26] Dynamic Bayesian inference can infer the time-evolving coupled dynamics in the presence of noise.[26] The interactions among frequency-specific oscillators can be studied effectively through their phase dynamics. To derive the coupling connections from the measured signals, a model of two coupled phased oscillators following the stochastic differential equation is defined as follows[26]:

$$\dot{\phi}_\iota(t) = w_i(t) + q_i\left(\phi_i, \phi_j, t\right) + \xi_i(t) \quad (1)$$

Where $i,j = \{1,2\}, i \neq j$ and $w_i(t)$ is the natural frequency. The function q_i of the two oscillators' phases ϕ_i and ϕ_j represents the coupling configuration. $\xi_i(t)$ denotes the Gaussian white noise. The deterministic periodic part of equation (1) can be Fourier decomposed into a sum of base functions $\Phi_k = \exp[I(k_1\varphi_1 + k_2\varphi_2 + \ldots + k_N\varphi_N)]$, which can be modulated by the time-varying bank of parameters $c_k^{(i)}$.

$$\dot{\phi}_\iota(t) = \Sigma_{K=-K}^{K} c_k^{(i)} \Phi_k\left(\phi_i, \phi_j, t\right) + \xi_i(t) \quad (2)$$

In this analysis, the order of Fourier expansion is $K = 2$. The rest of $c_k^{(i)}$ can be evaluated by DBI. The Fourier components Φ_k served as the base functions for inferring the coupling parameter $c_k^{(i)}$. c can be calculated recursively through a tutorial on time-evolving DBI and software codes.[26] The following four equations were used:

$$\mathrm{D} = \frac{h}{L}\left(\dot{\phi}_l - c_k\Phi_k\left(\phi^*_{.,l}\right)\right)^T\left(\dot{\phi}_l - c_k\Phi_k\left(\phi^*_{.,l}\right)\right) \quad (3)$$

$$\Gamma_w = \left(\Xi_{prior}\right)_{kw} c_w + h\Phi_k\left(\phi^*_{.,l}\right)\left(\mathrm{D}^{-1}\right)\dot{\phi}_l - \frac{h}{2}\frac{\sigma\Phi_k\left(\phi_{.,l}\right)}{\sigma\phi} \quad (4)$$

$$\Xi_{kw} = \left(\Xi_{prior}\right)_{kw} + h\Phi_k\left(\phi^*_{.,l}\right)\left(\mathrm{D}^{-1}\right)\Phi_w\left(\phi^*_{.,l}\right) \quad (5)$$

$$c_k = \left(\Xi^{-1}\right)_{kw}\Gamma_w \quad (6)$$

c of the coupled phase model was inferred by DBI, through which the coupling functions on a $2\pi \times 2\pi$ grid can be evaluated. The Euclidean norm of the inferred parameters from the

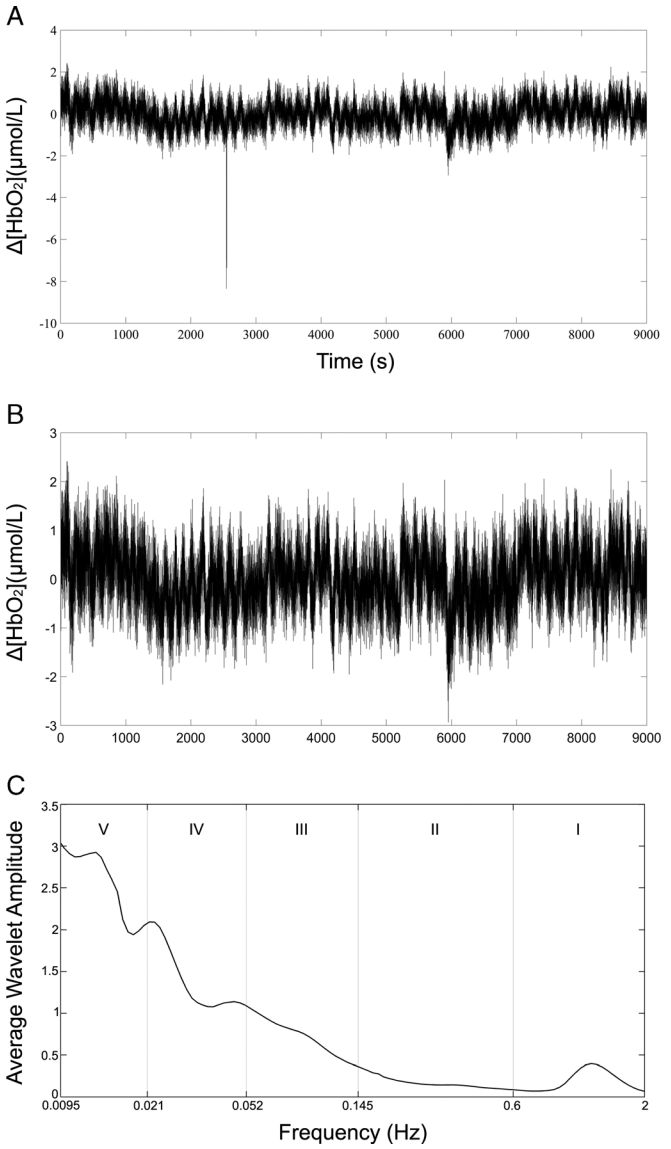

FIGURE 3. The original Δ[HbO_2] signal (A), the preprocessed Δ[HbO_2] signal (B), and the average wavelet amplitude in the five frequency intervals (C).

phase dynamics $\sigma_{i,j}$ is defined as the coupling strength (CS), which represents the influence exerted by oscillator *i* on oscillator *j*. Coupling strength is used to quantitatively describe the coupling interaction, which quantified the coupling amplitude.[26]

$$\sigma_{i,j} = \sqrt{\sum_{k=-k}^{k} \left(c_k^{(i:j)}\right)^2} \quad (7)$$

In this study, we reconstructed the coupling function between the Δ[HbO_2] signals in each frequency interval by using a model of coupled phase oscillators and DBI.

Kendall Correlation Analysis

The Kendall's τ rank correlation coefficient is a nonparametric statistic, which is used to measure the degree of correspondence between two rankings and assess the significance of this correspondence.[27] In this study, Kendall' analysis and τ co-efficiency were used to analyze the degree of correlation between the CS values and cognitive level (MMSE and MoCA scores).

Statistical Analysis

Normality (Kolmogorov-Smirnov' test) and homogeneity of variance (Levene' test) were used to ensure that CS values satisfy the assumption for parameter analysis. One-way analysis of variance was conducted to assess the effects of cognitive impairment on the CS levels in the MCI group. A difference of $P < 0.05$ was considered statistically significant.

RESULTS

Demographic Data

Subject information, including age, height, weight, body mass index, female sex, and blood pressure, is shown in Table 1.

TABLE 1. Basic information of the experimental subjects

Characteristic	MCI Group	Control Group	*P* for Difference
Age, yr	69.27 ± 3.64	70.15 ± 3.51	0.375
Height, cm	167.08 ± 10.09	166 ± 8.23	0.672
Weight, kg	63.62 ± 13.38	63.59 ± 11.27	0.995
Body mass index, kg/m^2	22.51 ± 2.21	22.89 ± 2.12	0.529
Systolic blood pressure, mm Hg	137.58 ± 25.32	123.71 ± 9.42	/
Diastolic blood pressure, mm Hg	85.35 ± 10.56	78.93 ± 7.92	/
Female sex, %	50	50	1
MMSE scores	26.15 ± 1.67	29.43 ± 0.5	/
MoCA scores	23.92 ± 1.29	26.68 ± 0.82	/

Values are presented as means with SDs and percentages. *P* values for differences are calculated using one-way analysis of variance for means and SDs and χ^2 test for percentages.

The two groups have similar age, body mass index, and sex ($P > 0.05$). Figures 4A and B show the comparisons of the MMSE and MoCA scores between the MCI and control groups, respectively.

Effective Connectivity

A total of 100 surrogate signals were generated by amplitude-adjusted Fourier transform for each channel to test the validity of CS values. Coupling strength was considered statistically significant only when the CS value from original signals had a value above the sum of its average surrogates' value plus two standard deviations in the same frequency interval.

Figures 5A and B show examples of the EC networks in intervals III and IV. A colored matrix box indicated a significant EC value between two channels, whereas a white matrix lattice represented an insignificant connection. Different colors denoted different values of CS. Figures 6A and 6B show the CS in intervals III and IV in the MCI and control groups. The CS levels of RPFC to LPFC ($F = 7.964$, $P = 0.007$), LPFC to ROL ($F = 4.278$, $P = 0.044$), and RPFC to LOL ($F = 4.429$, $P = 0.04$) in interval III as well as LPFC to LOL ($F = 5.637$, $P = 0.021$), ROL to LPFC ($F = 4.762$, $P = 0.034$), and RPFC to LOL ($F = 4.06$, $P = 0.049$) in interval IV in the MCI group were significantly lower than those in the control group. Figures 7A and B show examples of the EC networks of one MCI subject and one control subject, respectively. The MCI subject exhibited less connections in intervals III and IV than those of the control subject. Connections were observed among LPFC-LMC, LPFC-LOL, and LPFC-ROL in interval III in the control group, whereas no connection was found in these three types in the MCI subject. Connections were detected among LPFC-LOL and LMC-LOL in interval IV in the control group, whereas no connection was found in these two types in the MCI subject.

Correlation Analysis Between EC and Cognitive Performance

By Kendall analysis, strong positive correlations were observed between MMSE scores and the CS from LPFC to RPFC ($\tau = 0.575$, $P < 0.001$) and from RPFC to LPFC ($\tau = 0.395$, $P = 0.008$) in interval III, as well as from LPFC to RPFC ($\tau = 0.555$, $P < 0.001$) and from RPFC to LPFC ($\tau = 0.382$, $P = 0.01$) in interval IV.

Moreover, correlation analysis revealed that the MoCA scores were significantly positively correlated with the CS from LPFC to RPFC ($\tau = 0.533$, $P < 0.001$) and from RPFC to LPFC ($\tau = 0.355$, $P = 0.018$) in interval III, as well as from LPFC to RPFC ($\tau = 0.546$, $P < 0.001$) and from RPFC to LPFC ($\tau = 0.341$, $P = 0.023$) in interval IV.

DISCUSSION

In this study, several important findings were obtained. (1) The CS levels between the brain regions associated with

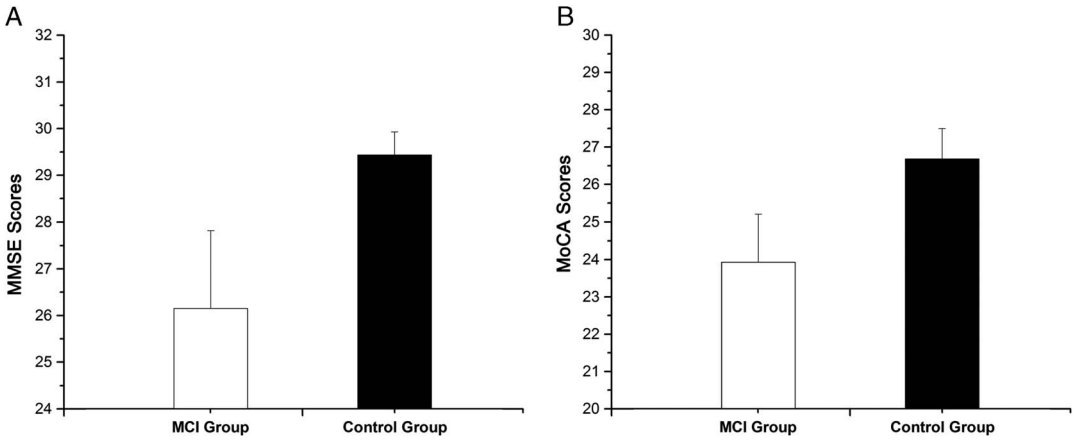

FIGURE 4. Comparisons of MMSE (A) and MoCA (B) scores between the MCI and control groups.

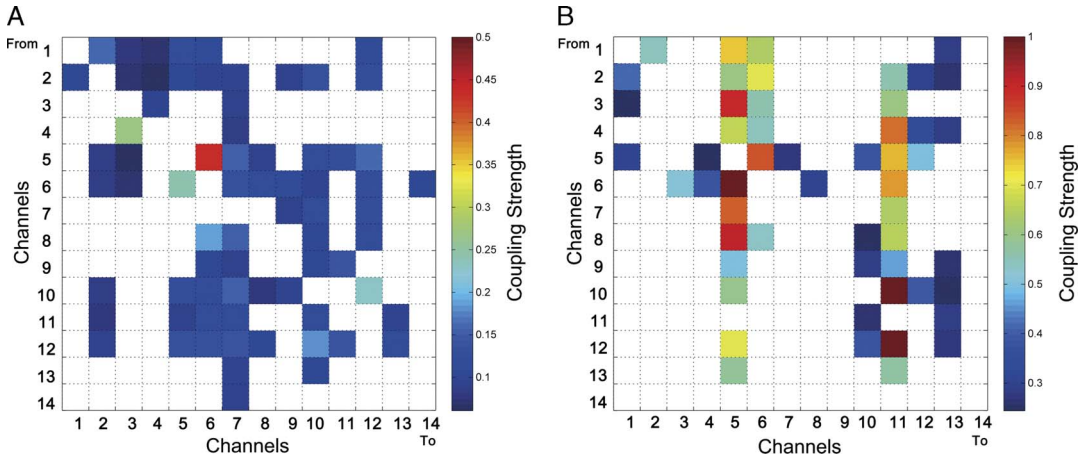

FIGURE 5. The mean CS matrix (number of channels: 14) of an MCI subject in interval III (A) and interval IV (B).

the prefrontal lobes in the MCI group were significantly lower than those in the control group. (2) The CS levels were closely related to cognitive performance (MMSE and MoCA scores).

Functional near-infrared spectroscopy can detect brain oxygen parameters in brain tissues. The activity of brain tissues can be indirectly obtained through the neurovascular coupling mechanism. Functional near-infrared spectroscopy is a blood oxygen-level–dependent technology. A strong correlation was found between the degree of cerebral nerve activity and the change of cerebral oxygen parameters.[15] Cerebral oxygenation signals measured by fNIRS are composed of neurovascular coupling and systemic activity components.[15] In this study,

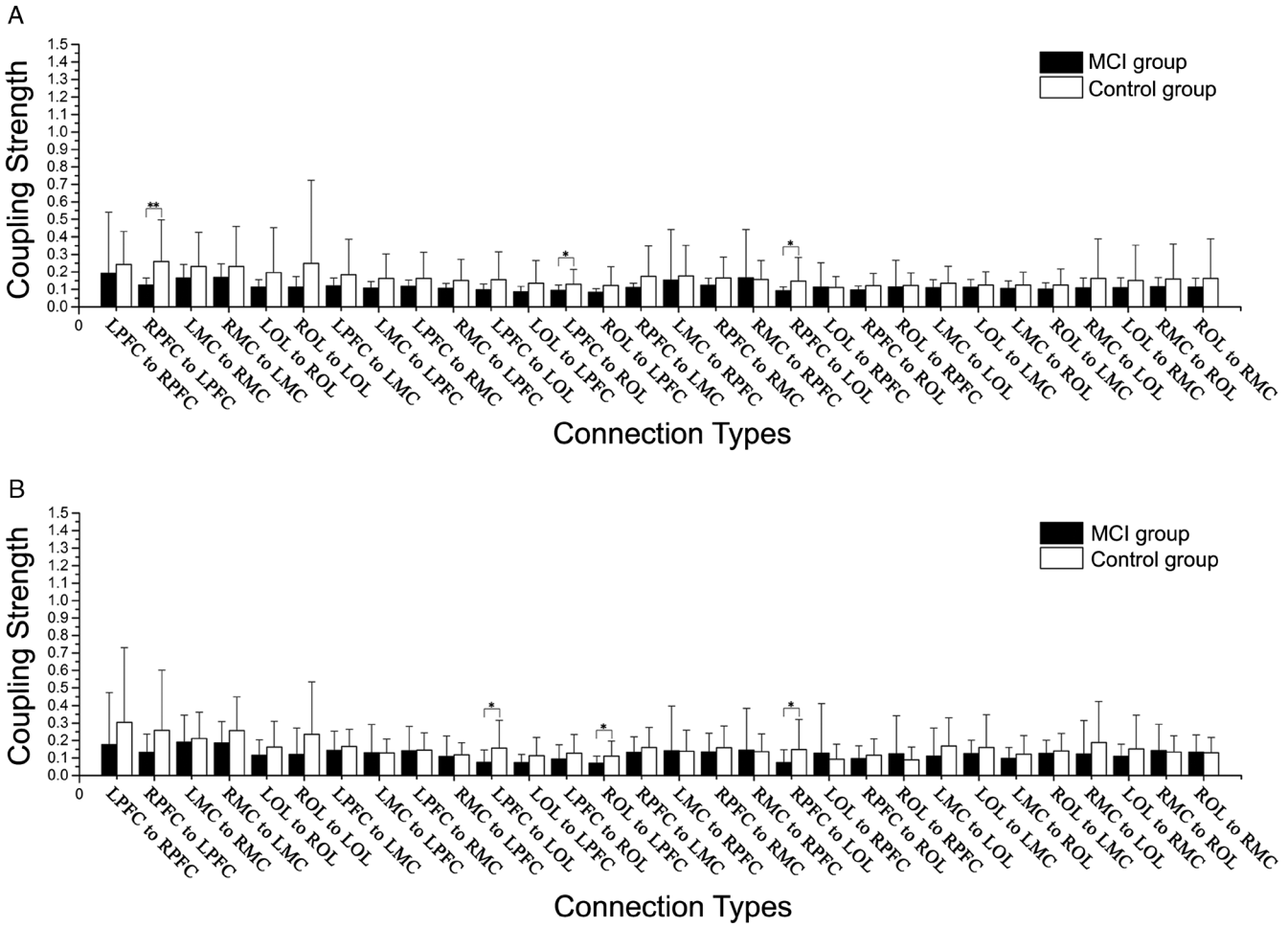

FIGURE 6. Comparisons of CS in intervals III and IV in the 30 connectivity types. A, MCI and control groups in interval III. B, MCI and control groups in interval IV. Significant differences are marked with $*P < 0.05$ and $**P < 0.01$.

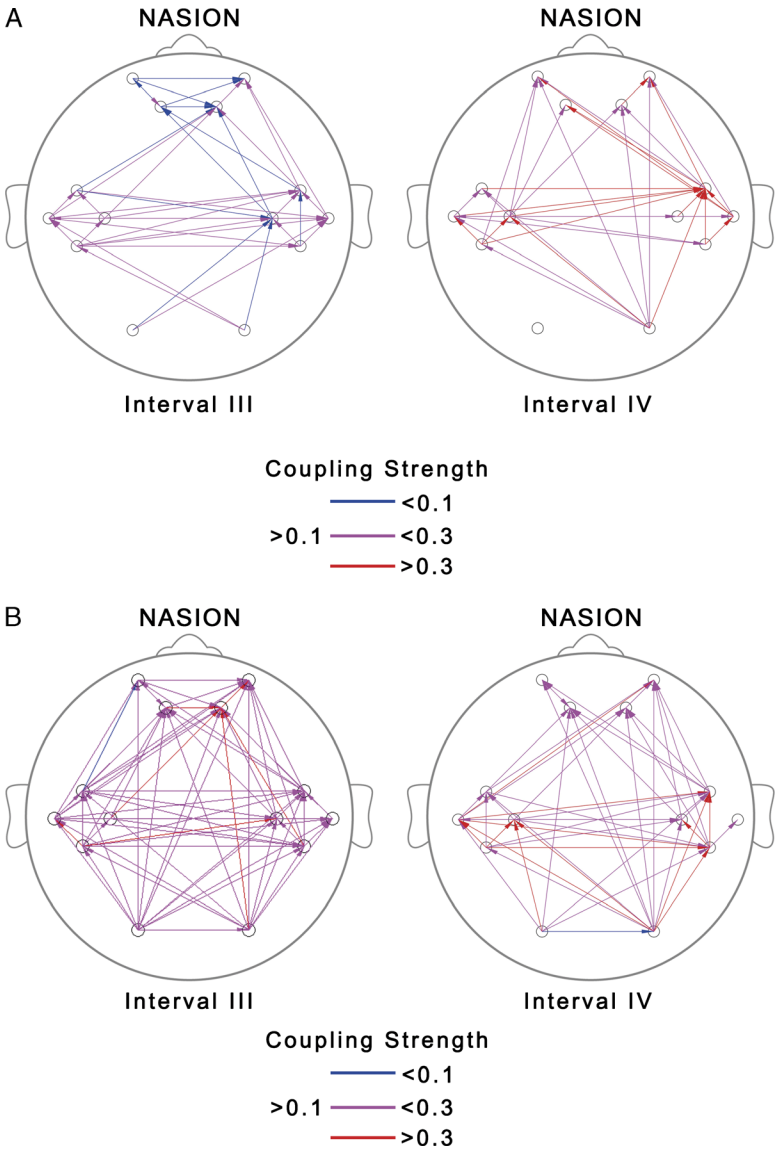

FIGURE 7. Examples of the EC network of one MCI subject (A) and one control subject (B).

the EC was calculated in five frequency intervals (I: 0.6–2 Hz; II: 0.145–0.6 Hz; III: 0.052–0.145 Hz; IV: 0.021–0.052 Hz; V: 0.0095–0.021 Hz), which reflect the neurovascular coupling and systemic activity components.[25]

The driving relationships among different brain regions and the direction of the relationships are reflected by the main coupling direction. The CS levels of RPFC to LPFC, LPFC to ROL, and RPFC to LOL in interval III showed significantly lower levels in the MCI group than in the control group. The blood oxygen fluctuation in frequency interval III was presumed to reflect myogenic activity that originated locally from the intrinsic myogenic activity of smooth muscle cells in resistance vessels.[25] Vascular muscle cells provide active tension in the vessel wall and regulate the diameter of the vessels. Smooth muscle cells contract if the cell is stretched, and this mechanical stimulus triggers the depolarization of the membrane potential, causing the contraction of neighboring smooth muscle cells. This process provides a background pressure in the vessel and aids in blood transport.[25] Regulating the intrinsic myogenic activity of smooth muscle cells leads to imbalanced blood vessel dilation or contraction capacity on both sides of the forehead, which may significantly reduce the CS levels. The efficiency of information transmission was reduced from RPFC to LPFC, LPFC to ROL, and RPFC to LOL in interval III, and this may be attributed to the imbalance in myogenic activity regulation among these areas. The previous functional magnetic resonance imaging study revealed that the EC in the default mode network was altered in MCI patients, including a decreased EC in the middle temporal gyrus, hippocampus, fusiform gyrus, and between the precuneus/posterior cingulate cortex and the hippocampus.[28] Moreover, another functional magnetic resonance imaging study demonstrated that neural network interactions differ markedly between MCI patients and healthy older adults.[29] Our current findings were consistent with these previously mentioned results.

Another interesting finding is that the CS levels in interval IV significantly varied between the MCI and control groups. A study reported that at this frequency interval, hemodynamic

parameters were regulated through tight neurovascular coupling and partial autonomic control.[30] The CS levels of LPFC to LOL, ROL to LPFC, and RPFC to LOL in interval IV in the MCI group were significantly lower than those in the control group. The parasympathetic and sympathetic nervous systems are two kinds of autonomic nervous systems that affect the heart's activities.[25] A novel EC network estimation study showed that the EC for most of the optimal connections is much sparser in MCI group than that in control group.[10]

Brain regions with reduced CS mostly appeared in the prefrontal cortex–related brain regions. The prefrontal cortex is closely related to cognitive function, and the decrease in the CS among prefrontal cortex–related brain regions reflected the decline in the transmission efficiency of this part of the connection. The decrease in cognitive function in MCI may be related to the reduction of CS among these brain regions.

The intersubject variation exists on the channel-wise EC network. Through the surrogate test, significant connections were determined in the network. In this study, we aimed to analyze the changes related to the MCI in directed interactions among the brain regions. The CS values of significant interactions were averaged for 30 directed interregional connection types between all possible pairs of 14 channels in each subject, and thereby, the mutual interactions were analyzed among the six regions. The region-wise interactions are LPFC to RPFC, RPFC to LPFC, LPFC to LMC, LMC to LPFC, LPFC to RMC, RMC to LPFC, LPFC to LOL, LOL to LPFC, LPFC to ROL, ROL to LPFC, RPFC to LMC, LMC to RPFC, RPFC to RMC, RMC to RPFC, RPFC to LOL, LOL to RPFC, RPFC to ROL, ROL to RPFC, LMC to RMC, RMC to LMC, LMC to LOL, LOL to LMC, LMC to ROL, ROL to LMC, RMC to LOL, LOL to RMC, RMC to ROL, ROL to RMC, LOL to ROL, and LOL to ROL, respectively.

Limitations

Cerebral oxygenation signals measured by fNIRS are known to have systemic interferences, which is a limitation of this study. Short-channel or spatial regression will be applied to separate the effect in further study. Another limitation of this study is the interference of Mayer waves (0.08–0.1 Hz). Mayer waves are oscillations of arterial pressure occurring spontaneously in conscious subjects, which are tightly coupled with the synchronized oscillations of efferent sympathetic nervous activity. The quality of the study will be improved with systemic measurement (such as heart rate, blood pressure, and breathing rate measurements).

CONCLUSIONS

This study used the DBI to calculate the brain EC through fNIRS and analyzed the frequency-specific brain EC of MCI subjects under resting state. Significantly decreased interregional EC was found in intervals III and IV in the MCI group as compared with that in the control group. The decreased connectivity in intervals III and IV was also strongly positively correlated with cognitive performance in the MCI subjects. This method has potential for the assessment of MCI subjects and for further expansion of rehabilitation training.

REFERENCES

1. Tuokko HA, Mcdowell I: An overview of mild cognitive impairment. *New Engl J Med* 2006;356:1175
2. Carlo AD, Lamassa M, Baldereschi M, et al: CIND and MCI in the Italian elderly: frequency, vascular risk factors, progression to dementia. *Neurology* 2007;68:2186–7
3. Petersen RC: Mild cognitive impairment as a diagnostic entity. *J Intern Med* 2004;256:183–94
4. Mcgough EL, Kelly VE, Weaver KE, et al: Limbic and basal ganglia neuroanatomical correlates of gait and executive function: older adults with mild cognitive impairment and intact cognition. *Am J Phys Med Rehabil* 2018;97:229–35
5. Stokholm J, Vogel A, Gade A, et al: Heterogeneity in executive impairment in patients with very mild Alzheimer's disease. *Dement Geriatr Cogn Disord* 2006;22:54–9
6. Nasreddine ZS, Phillips NA, Bédirian V, et al: The Montreal Cognitive Assessment, MoCA: a brief screening tool for mild cognitive impairment. *J Am Geriatr Soc* 2005;53:695–9
7. Ramlall S, Chipps J, Bhigjee AI, et al: The sensitivity and specificity of subjective memory complaints and the subjective memory rating scale, deterioration cognitive observee, mini-mental state examination, six-item screener and clock drawing test in dementia screening. *Dement Geriatr Cogn Disord* 2013;36:119–35
8. Yamamoto S, Mogi N, Umegaki H, et al: The clock drawing test as a valid screening method for mild cognitive impairment. *Dement Geriatr Cogn Disord* 2004;18:172–9
9. Kalbe E, Kessler J, Calabrese P, et al: DemTect: a new, sensitive cognitive screening test to support the diagnosis of mild cognitive impairment and early dementia. *Int J Geriatr Psychiatry* 2004;19:136–43
10. Li Y, Yang H, Li K, et al: *Novel effective connectivity network inference for MCI identification*. Paper presented at International Workshop on Machine Learning in Medical Imaging, Quebec, Canada, September 10, 2017
11. Morbelli S, Brugnolo A, Bossert I, et al: Visual versus semi-quantitative analysis of 18F-FDG-PET in amnestic MCI: an European Alzheimer's Disease Consortium (EADC) project. *J Alzheimers Di Jad* 2015;44:815–26
12. Petersen RC: Mild cognitive impairment. *New Engl J Med* 2011;364:2227–34
13. Biswal B, Yetkin FZ, Haughton VM, et al: Functional connectivity in the motor cortex of resting human brain using echo-planar MRI. *Magn Reson Med* 1995;34:537–41
14. Friston KJ: Functional and effective connectivity: a review. *Brain Connect* 2011;1:13–36
15. Scholkmann F, Kleiser S, Metz AJ, et al: A review on continuous wave functional near-infrared spectroscopy and imaging instrumentation and methodology. *Neuroimage* 2014;85(pt 1):6–27
16. Miller EK, Cohen JD: An integrative theory of prefrontal cortex function. *Annu Rev Neurosci* 2001;24:167–202
17. Hogenhout M: The age-related regulation of sensorimotor integration in human postural control. *Mol Cell Biol* 2013;8:4889–95
18. Astafiev SV, Stanley CM, Shulman GL, et al: Extrastriate body area in human occipital cortex responds to the performance of motor actions. *Nat Neurosci* 2004;7:542–8
19. Faul F, Erdfelder E, Lang AG, et al: G*Power 3: a flexible statistical power analysis program for the social, behavioral, and biomedical sciences. *Behav Res Methods* 2007;39:175–91
20. Cameron JD, Gallagher R, Pressler SJ, et al: Sensitivity and specificity of a five-minute cognitive screening test in patients with heart failure. *J Card Fail* 2016;22:99–107
21. Bu L, Wang D, Huo C, et al: Effects of poor sleep quality on brain functional connectivity revealed by wavelet-based coherence analysis using NIRS methods in elderly subjects. *Neurosci Lett* 2018;668:108–14
22. Bu L, Huo C, Xu G, et al: Alteration in brain functional and effective connectivity in subjects with hypertension. *Front Physiol* 2018;9:1–12
23. Scholkmann F, Spichtig S, Muehlemann T, et al: How to detect and reduce movement artifacts in near-infrared imaging using moving standard deviation and spline interpolation. *Physiol Meas* 2010;31:649
24. Bu L, Li J, Li F, et al: Wavelet coherence analysis of cerebral oxygenation signals measured by near-infrared spectroscopy in sailors: an exploratory, experimental study. *BMJ Open* 2016;6: e013357
25. Shiogai Y, Stefanovska A, Mcclintock PV: Nonlinear dynamics of cardiovascular ageing. *Phys Rep* 2010;488:51–110
26. Stankovski T, Duggento A, Mcclintock PVE, et al: A tutorial on time-evolving dynamical Bayesian inference. *Eur Phys J Spec Top* 2014;223:2685–703
27. Bolboac SD, Jantschi L: Pearson versus Spearman, Kendall's Tau correlation analysis on structure-activity relationships of biologic active compounds. *Leonardo J Sci* 2006;5: 179–200
28. Yan H, Zhang Y, Chen H, et al: Altered effective connectivity of the default mode network in resting-state amnestic type mild cognitive impairment. *J Int Neuropsychol Soc* 2013;19:400–9
29. Hampstead BM, Khoshnoodi M, Yan W, et al: Patterns of effective connectivity during memory encoding and retrieval differ between patients with mild cognitive impairment and healthy older adults. *Neuroimage* 2015;124(pt A):997–1008
30. Zhang R, Zuckerman JH, Iwasaki K, et al: Autonomic neural control of dynamic cerebral autoregulation in humans. *Circulation* 2002;106:1814–20